Morphology and depth of reflectors from 2D non-linear inversion of seismic data

M. Vassallo[1], V. Nisii[2], A. Zollo[1], G. Iannaccone[2]
[1] *Dipartimento di Scienze Fisiche, Università Federico II di Napoli*
[2] *Osservatorio Vesuviano, INGV, Napoli*

Abstract: We present here two methods to obtain reflection images of upper crust seismic reflectors. The techniques are based on migration and waveform coherence analysis of reflected seismic phases recorded in local earthquake seismograms and in active seismic data.
The first method is a move-out and stack of reflected seismic phases in local earthquake recordings. The theoretical travel times of reflected/converted phases in a 1D medium for a given interface depth and velocity model are used to align the recordings in time. The locations and origin times of events are initially estimated from the P and S arrival times. Different seismic gathers are obtained for each reflected/converted phase at the interface under consideration, and the best interface depth is chosen as that which maximizes the value of a semblance function computed on moved-out records. This method has been applied to seismic records of microearthquakes that have occurred at the Mt. Vesuvius volcano, and it confirms the reports of an 8- to 10-km-deep seismic discontinuity beneath the volcano that was previously identified as the roof of an extended magmatic sill.
The second is a non-linear 2D method for the inversion of reflection travel times aimed at the imaging of a target upper-crust reflector. This method is specifically designed for geophysical investigations in complex geological environments (oil investigations, retrieving of images of volcano structures) where the presence of complex structures makes the standard velocity analysis difficult and degrades the quality of migrated images. Our reflector is represented by nodes of a cubic-spline that are equally spaced at fixed horizontal locations. The method is based on a multiscale approach and uses a global optimization technique (genetic algorithm) that explores the whole of the parameter space, i.e. the interface position nodes. The forward problem (the modelling of reflection travel times) is solved using the finite-difference solver of Podvine & Lecomte (1991) and using an *a priori* known background velocity model. This non-linear method allows the automated determination of the global minimum (or maximum) without relying on estimates of the gradient of the objective function in the starting model and without making assumptions about the nature of the objective function itself. We have used two types of objective functions. The first is a least-squares L2 norm, defined as the sum of the squared differences

between the observed and the calculated travel times. The second is based on coherence measures (semblance). The main advantage of using coherence measures is that they do not require travel-time picking to assess the degree of fit to the data model. Thus, the time performance of the whole procedure is improved and the subjectivity of the human operators in the picking procedure is removed.
The methods are tested on synthetic models and have been applied to a subset of data that was collected during the active seismic experiments performed in September 2001 in the gulfs of Naples and Pozzuoli in the framework of what is known as the SERAPIS project.

Introduction

Reflected and/or converted phases from crustal discontinuities have been frequently observed on microearthquake records (Iyer, 1992). The analysis of secondary arrivals using different techniques has proven to be valuable for the definition of the position and physical characteristics of reflecting interfaces. The modelling of reflected and/or converted waves is widely used for the retrieving of other physical parameters of the propagation medium in seismic exploration (P-to-S impedance contrast, anisotropy, P-to-S velocity ratio, and others) (Yilmaz, 1987; Sheriff and Geldart, 1982).
Recently, several studies of wave amplitudes and arrival times of secondary wave trains on earthquake recordings have been used to study the crustal structure (James et al., 1987) and to delineate the geometry and extension of a magmatic body in various volcanic regions. For example, the use of travel-time and amplitude analyses for the location and interpretation of S-to-S and P-to-S reflected phases from a local seismic network in the area of Socorro, Rio Grande Rift (New Mexico, USA), allowed the identification of a sharp crustal discontinuity at a depth of approximately 18 km, which was interpreted as the top of a thin, extended magma layer (Sanford et al., 1973; Rinehart et al., 1981; Balch et al., 1997). Other evidence for mid-crust discontinuities of magmatic origin have been found in Japan, at the Nikko-Shirane volcano (Matsumoto and Hasegawa, 1996) and in California, at the Long Valley caldera (Stroujkova and Malin, 2000) through the analysis of S-to-S and S-to-P waves observed on microearthquake records.
In the present study, we first search for deeper discontinuities beneath Mt. Vesuvius by using the move-out and stacking method that is usually applied in exploration seismology and that is known as a coherency stack (Naess and Burland, 1985). Based on an *a priori* known background velocity model, the optimal interface depth is determined by maximizing the semblance function, which is calculated from the converted and reflected phase signals extracted from the microearthquake records (Nisii et al., 2004).
Determination of geological discontinuities from active seismic data is usually carried out by migration techniques (Yilmaz and Chambers, 1984; Yilmaz,

1987; Sheriff and Geldart, 1982) that require prior knowledge of the velocity. Conventional velocity analysis methods, such as semblance analysis (Toldi 1989), focusing analysis (Yilmaz and Chambers, 1984), and migration move-out analysis (Al-Yahya, 1989), are carried out interactively. However, in complex geological environments, the presence of complex structures makes the standard velocity analysis difficult and degrades the quality of migrated images. Another approach is to use the inversion of reflection data: first, a high resolution velocity model is determined by first-arrival travel time inversion, and then this model is used as the background reference medium for an interface inversion that is aimed at imaging a target reflector (Amand & Virieux 1995, Improta 2002).

In this study, we examine the use of a non-linear optimization method to obtain the localization and morphology of a seismic reflector by using active seismic data. The inversion method is designed to image rough reflectors that are embedded in an *a priori* known, laterally inhomogeneous velocity model. This method is based on the simulation of seismic wave propagation in a given media, and it employs a scheme of non-linear optimisation for the determination of the interface model. For a given interface model, the data are calculated with numerical techniques (forward problem) and the reliability of the model is evaluated by means of a cost-function value that is defined by the difference between the observed and the calculated data. Then, the interface model determination becomes a numerical determination of the minimal-cost model (optimization). The method is specifically designed for geophysical investigations in complex geological environments, for the obtaining of the morphology and the positions of embedded discontinuities.

We envision that these kinds of techniques will be appropriate as part of much more comprehensive investigations where the crustal velocities and regional structures can be determined by a variety of methods that involve controlled as well as natural sources.

Modelling of reflected/converted arrival time phases in local earthquake recordings. Application to the Mt. Vesuvius data

Method 1

The proposed method to model the reflected/converted arrival times follows the approach usually used in reflection seismology for the determination of the morphology of reflecting interfaces by means of the post-stack migration of seismic sections.

Assuming a horizontal reflector in a medium with a given 1D background velocity model, the theoretical arrival times of the four possible reflected/con-

verted phases are calculated (P-to-P, S-to-P, S-to-S, P-to-S) for any source and receiver pair of the analyzed waveform data set. For each considered wave type, a time window on the seismic records is centred on the theoretical arrival time. The semblance function is calculated in the selected time windows for all of the records along the entire seismic section. The semblance, S_T, is defined as the ratio of the total energy of the stacked trace in the time interval $(t+\Delta t)$ to the sum of the energies of the individual traces in the same time interval (Neidell and Taner, 1971):

$$S_T = \frac{1}{N} \frac{\sum_{t}^{t+\Delta t} \left(\sum_{i=1}^{N} g_{ti} \right)^2}{\sum_{t}^{t+\Delta t} \sum_{i=1}^{N} (g_{ti})^2} \tag{1}$$

where g_{ti} is the amplitude of trace *i* at time *t*. The semblance range of variability is between 0 and 1. The semblance is a measure of the wave-form similarity between different seismic records. For very coherent events in different records, this function assumes values close to 1. Prior to the computation of the semblance, the seismic records were normalized to minimize the differences arising from varying source magnitudes.

The semblance is evaluated for a given range of interface depths, and for each interface depth, different time windows are selected on the seismograms according to the newly computed phase arrival times. The optimal interface depth is selected as the one which maximizes the semblance for each of the analyzed reflections and converted events.

Assuming that the background velocity model is correct, a well-identified reflection/conversion event must generate pulses aligned at the zero time value in a moved-out seismic section. The alignment can be quantitatively verified by computing the stack function versus time (i.e. the sum of the amplitude at any time along the seismograms in the entire seismic section). The presence of reflected/converted arrivals in the section will correspond to a peaked stack function, with its maximum at time zero.

The method can be applied to the search of different secondary waves (P-to-P, P-to-S, S-to-P, S-to-S) on three-component seismograms. The comparisons of the semblance and stack plots calculated for the different phases allows for better constraint of the interface depth. The method assumes an *a priori* knowledge of the earthquake hypocentres and the background velocity model, which is assumed to be one dimensional. The uncertainty of these parameters may strongly affect the phase identification in seismograms and the correct positioning of the depth of the interface. In addition, other effects can bias the interface location, such as station statics (including topographical effects), and possible 3D heterogeneity of the propagation medium and an irregular morphology of the interface.

Application

We have applied this described method to the interpretation of the vertical component records from 24 local seismic events that occurred between July and December of 1999 and that were recorded by the surveillance network operated by Osservatorio Vesuviano, INGV. The duration magnitudes ranged from 0.4 to 3.0. A total number of 205 vertical component recordings were selected for the present study. The events were located in a 3D velocity model (Lomax et al., 2001) using the non-linear technique proposed by Lomax et al. (2000). The resulting hypocentres lie along the axial zone of the volcano edifice in the depth range of 1-4 km. The final epicentral distances between events and stations vary between a few hundred meters to 17 km (Figure 1). The calculated travel-time RMS values are smaller than 0.1 s.

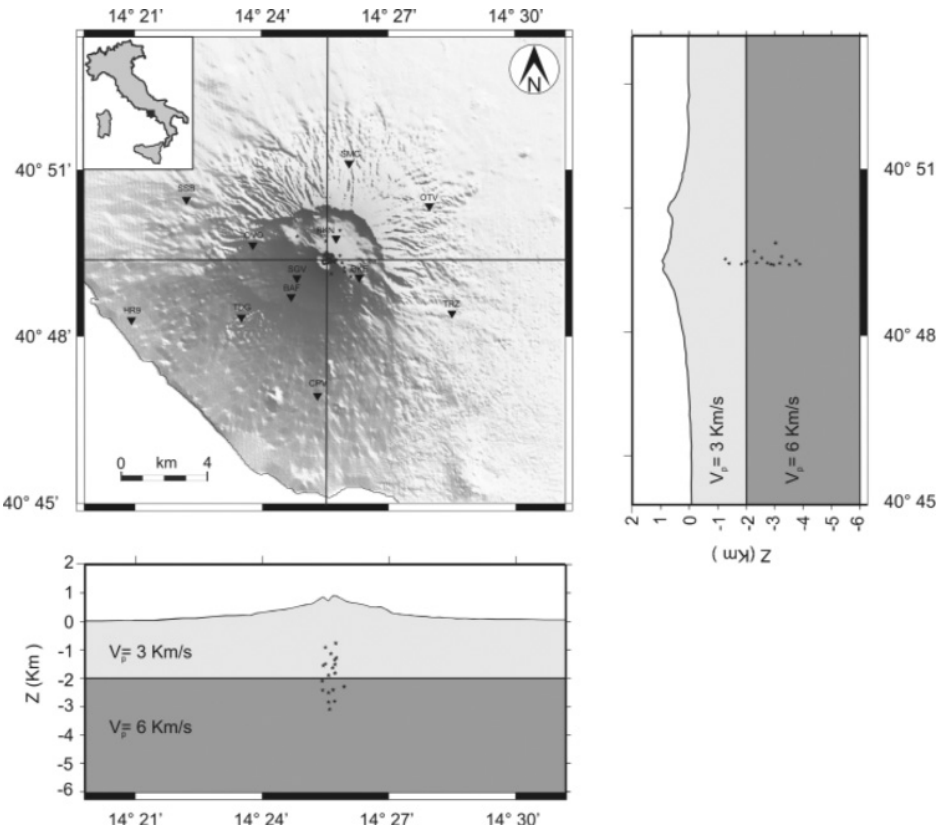

Fig. 1. Topographical map showing Mt Vesuvius and some of the seismic stations of the surveillance network owned by Osservatorio Vesuviano, INGV (solid triangles). The North-South and East-West vertical cross-sections show the 24 local event positions (stars) selected, and the assumed 1D velocity models.

The study of the converted/reflected waves was carried out considering a reflector depth ranging from 4 to 15 km with 0.2-km depth intervals. The minimum depth value was chosen as being deeper than the discontinuity between the alluvial and the recent volcanic sediments and the Mesozoic limestone formations, the average depth of which was determined to be 2 km (Zollo et al., 2002b).
The assumed background velocity model is composed of one layer over a half space (Zollo et al., 2002a; Lomax et al., 2001) (Figure 1). The calculation of the arrival times of the reflected phases was carried out by a two-point ray-tracing technique in the layered velocity model. Only the P-to-P and S-to-P wave types were considered for the analysis, since they are the most readable on the vertical component seismograms. A time window of 0.2 s centred at the theoretical arrival time of the reflected/converted phase was chosen. For more details of the data pre-processing adopted to reduce uncertainties associated with the use of local earthquake recordings, see Nisii et al. (2004).
The analysis of the semblance as a function of the interface depth for the P-to-P phase showed a major coherence value at about 9 km. A similar depth was obtained from the S-to-P phase analysis. The P-to-P phases identified by the semblance method are clearly visible in seismograms arranged as a common shot gathered in a conventional seismic reflection section (Figure 2). The records were moved-out according to the theoretical arrival times of a P-to-P phase for an interface depth of 9 km. The reflected wave pulses align around time zero on the moved-out section in Figure 2. The records of the stack and semblance as a function of time confirm the evidence of a secondary arrival

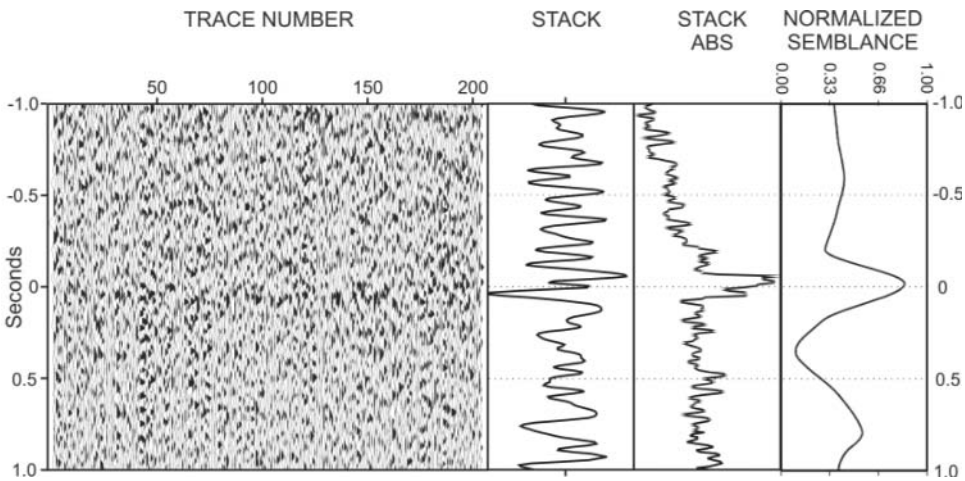

Fig. 2. An example of the seismograms showing clear secondary arrivals. The zero time is the origin time of the microearthquakes. The solid markers indicate the theoretical arrival times of the direct S wave and of the reflected/converted P-to-P and S-to-P phases from an interface at about 9 km in depth. The traces have been normalized to the integral of ABS.

with the presence of a marked peak at time zero. A quantitative estimation of the interface depth was provided by the time width of the semblance function around zero time in Figure 2. A total time width of about 0.3 s was measured for the P-to-P phases, which assumes a velocity of 6 km/s above the interface, suggesting an uncertainty of about 1 km for the interface depth.
The main sources of error affecting the width of the semblance can be the uncertainty in the earthquake location (hypocentral coordinates and origin time), a non-planar shape of the reflecting interface, and lateral heterogeneity of the velocity model. In the case of the Mt. Vesuvius earthquakes, assuming a realistic variability for all of these unknown parameters, the observed variation in the arrival time of reflected/converted phases is much smaller than the average wave travel time from sources to the receivers (tenths of seconds vs several seconds). This is the reason that despite the simplicity of the propagation model, a satisfactory alignment of the reflected/converted phases can be obtained, with a small dispersion around the zero time value in the seismic section.

MORPHOLOGY AND DEPTH OF REFLECTORS FROM 2D NON-LINEAR INVERSION OF ACTIVE SEISMIC DATA

Method 2

This method is based on the same concept as the previous one, but it is applied to active seismic data to obtain the depth and the morphology of an interface embedded in 2D heterogeneous media.
The reflection travel times are calculated by a three-step procedure. Initially, the first arrival travel times from each source and receiver to the nodes of a regular grid are calculated by the fast-time estimator of Podvin & Lecomte (1991). These travel times are calculated for a velocity model that has the same velocity values as the background model up the interface, and a velocity of zero below the interface (Figure 3); in this mode, only the reflected travel times are considered in the process. Then, the one-way travel times for each source/receiver to each point of the interface are calculated through an interpolation among the nearest four grid nodes (Figure 3). Finally, according to Fermat's principle, the reflection point for a source-receiver pair and for a given interface will be that which provides the minimum total travel time.
The reflector is represented by a cubic-spline function where the control points are equally spaced in the horizontal direction at fixed horizontal locations, and they can move vertically with continuity within a given depth range. The inversion is based on the numerical optimization of two possible cost functions. The first is a least squares L_2 norm, defined as the sum of the squared differences between the observed and the theoretical travel times. The second cost function is based on the value of the semblance (Neidell and Taner, 1971) that is evaluated along the calculated travel-time curves. For any source-

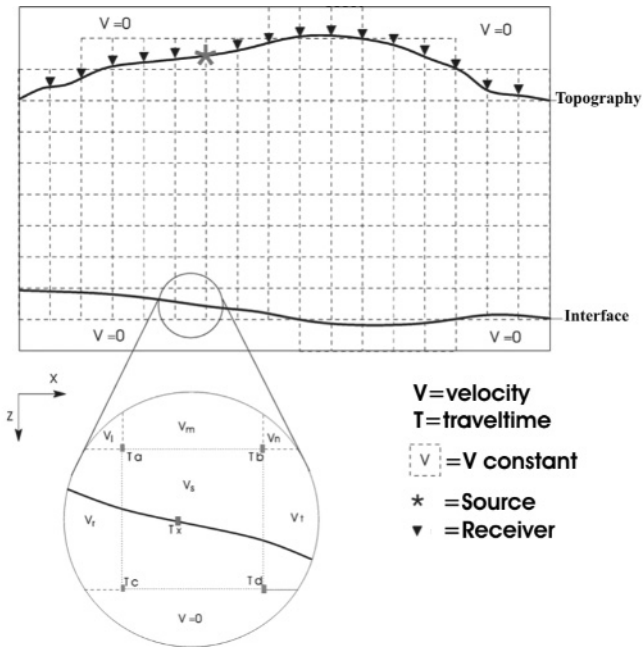

Fig. 3. Scheme followed for the resolution of the forward problem. The velocity model is divided into constant velocity boxes with a regular grid. In the grid nodes, the travel times are calculated by the Podvine & Lecomte (1991) finite differences method. The large circle shows a magnification of the Figure: the travel time in a fixed interface point (dots on the curve) is evaluated by performing an interpolation among the nearest four grid nodes (dots on the square).

receiver pair, a time window that is centred at the theoretical arrival time is selected on the seismic records. The semblance function (1) is computed in the selected time windows for all of the records along the entire seismic section (Figure 4). The semblance is a measure of the reflection/conversion waveform similarity. The main advantage of using wave-form coherence is that it does not require travel-time phase picking, thus improving the time performance of the whole procedure and removing the effects caused by the subjectivity of the human operators in the picking procedure.

The inversion strategy follows a multiscale approach (Lutter & Nowack, 1990): a series of inversions is run by progressively increasing the number of interface nodes. The strategy is described by the following steps:

1. With a minimal number of parameters fixed, the interface model is determined without putting ties on the dimension of the parameter space;
2. A model characterized from a greater number of parameters is searched for in the neighbourhood of the solution previously found;
3. The successive inversion run uses the same technique: the model, defined from a greater number of parameters is searched in the neighbourhood of the model previously determined.

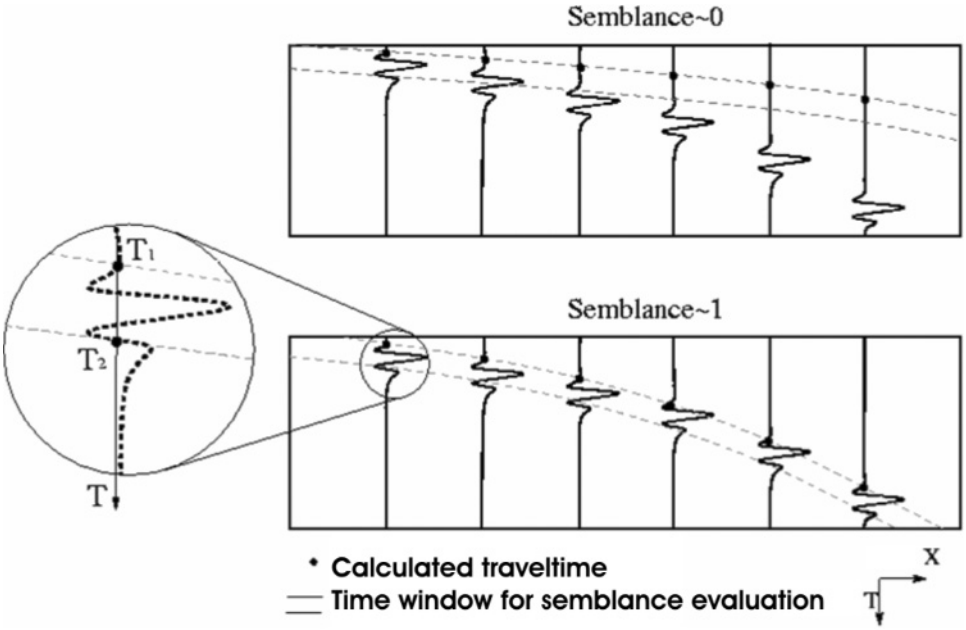

Fig. 4. Semblance evaluation along two different travel-time curves. For the calculation of the semblance, we extract the waveform contents in the windows given by the calculated travel times (in the large circle, the window is between the times T_1 and T_2). In the upper box, a bad travel time curve is shown (low semblance value), while the lower panel shows a travel-time curve that followed a coherent phase (high semblance value).
You can see this figure in color on page 219.

In this way, the passage from one step to the successive step improves the small wavelength characteristics of the final reflector model.
The search for the model parameter vector that minimizes the cost function (or maximizes the semblance function) is performed through the technique of the genetic algorithm (GA; Goldberg 1989; Whitley 1994) optimization method. Among the different non-linear optimization methods (Monte Carlo, simulated annealing), the GA has been shown to be very efficient and fast for the wide exploration of a multi-parametric model space and for the bracketing of the region containing the absolute minimum (Boschetti et al., 1996; Sambridge and Drijkoningen, 1992).

Application to simulated data

In this section, we present the results of our trials of the non-linear inversion on the synthetic models. The inversion of numerical simulated data is very important because it provides information about the ability of the method for the retrieval of the fixed geometrical features used to obtain the synthetic

dataset. We have performed two different simulated inversions. The first is based on the optimization of the L_2 norm, where the simulated data are the reflected travel times calculated on a fixed propagation media width of a given reflector. In the second, the inversion is based on the maximization of the semblance function, where the simulated data are the seismogram-calculated width numerical method on a fixed propagation model.

L_2 TESTS

To obtain the synthetic reflected travel times, a 20-km long and 10-km deep model was used (Figure 5). The P-velocity (Vp) model is divided into two different sections by a curved reflector surface, with depths ranging from 5 km to 6 km. Between the topographic and reflector surfaces, the Vp increases with the depth; under the interface, the velocity is constant. Along the top of the model there are six sources and 14 receivers, thus resulting in 84 calculated travel times (Figure 5).

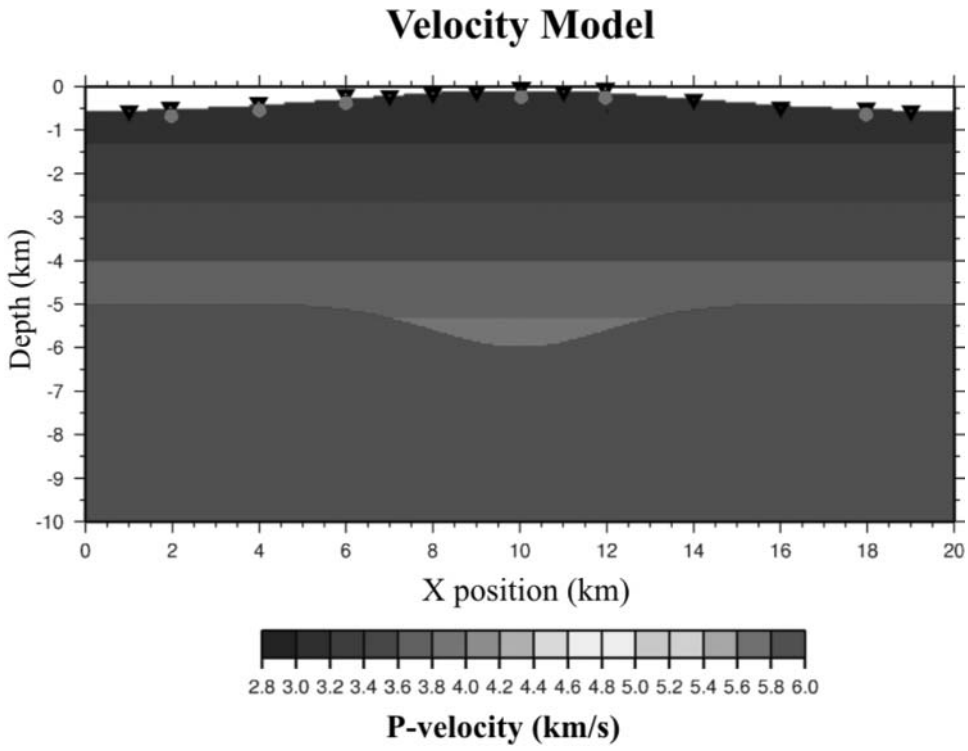

Fig. 5. Adopted model for the determination of synthetic travel times. The triangles show the locations of the receivers and the stars show the positions of sources.
You can see this figure in color on page 219.

For the first run, we allowed the node depth to vary from 0.5 km to 8.5 km. A succession of four interface models parametrized by 2, 3, 5 and 9 nodes were progressively inverted (Figure 6). Moving from a small to a larger number of interface position nodes, we always observed a decrease in the final cost function values and an increase in the agreement between the synthetic and the retrieved interface models. The RMS decreased from 0.14 s with the two-node model to 0.053 s for the final model (17-node model).

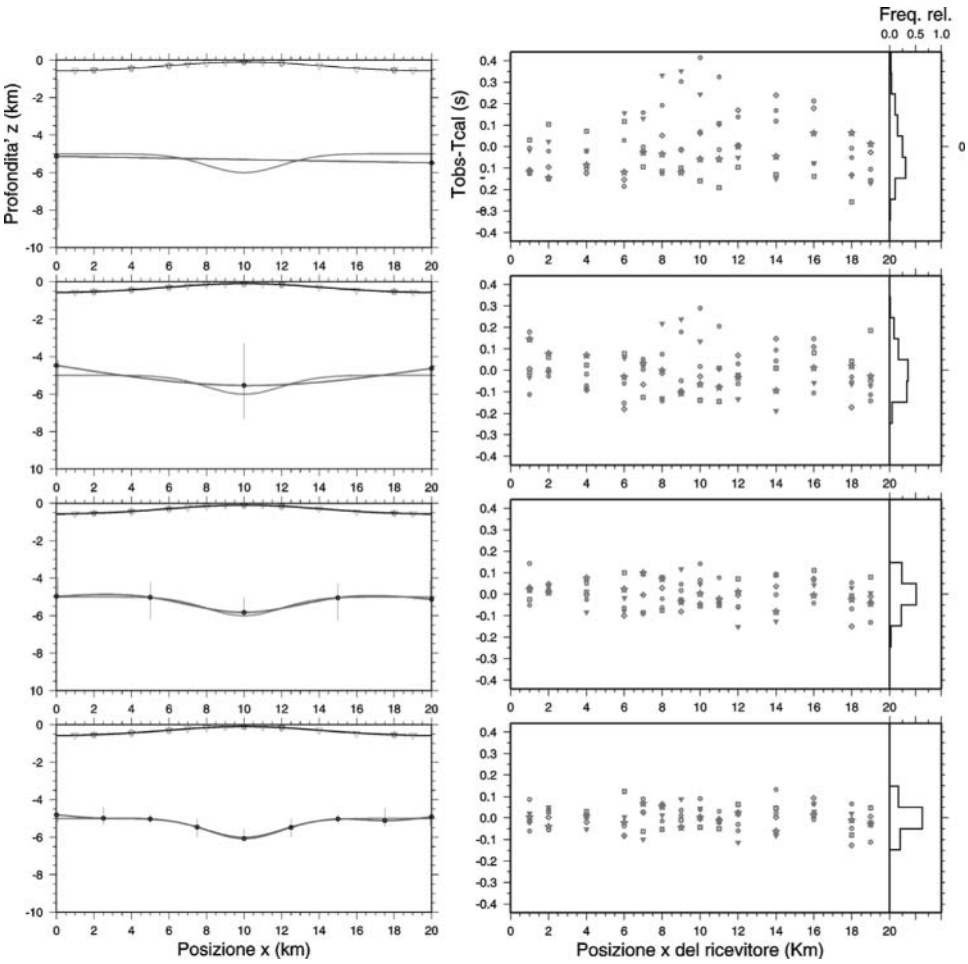

Fig. 6. The results of inversions of synthetic travel times. The final interface models are obtained by performing a succession of four inversion runs with an increasing number of interface nodes (solid circles). The line without nodes shows the real position of the reflector (Figure 5) and the vertical bars are the intervals of search of the nodes. In the panels on the right, the residual distributions and the histograms associated with determined models are displayed.
You can see this figure in color on page 220.

SEMBLANCE TEST

To test the inversion based on the waveform coherency criterion, we generated 150 synthetic seismograms that were obtained by the discrete wave-number method (Coutant, 1989). The seismograms were calculated using a propagation model formed of parallel and plane layers (Figure 7). In the first layer, the Vp was 3.5 km/s and the S velocity (Vs) was about 2.0 km/s; in the second layer, the Vp was 5 km/s and the Vs was 2.9 km/s. The interface that separates the two layers was located at 5 km of depth. Along the top of the model, there were two explosive sources and 75 receivers (Figure 7).

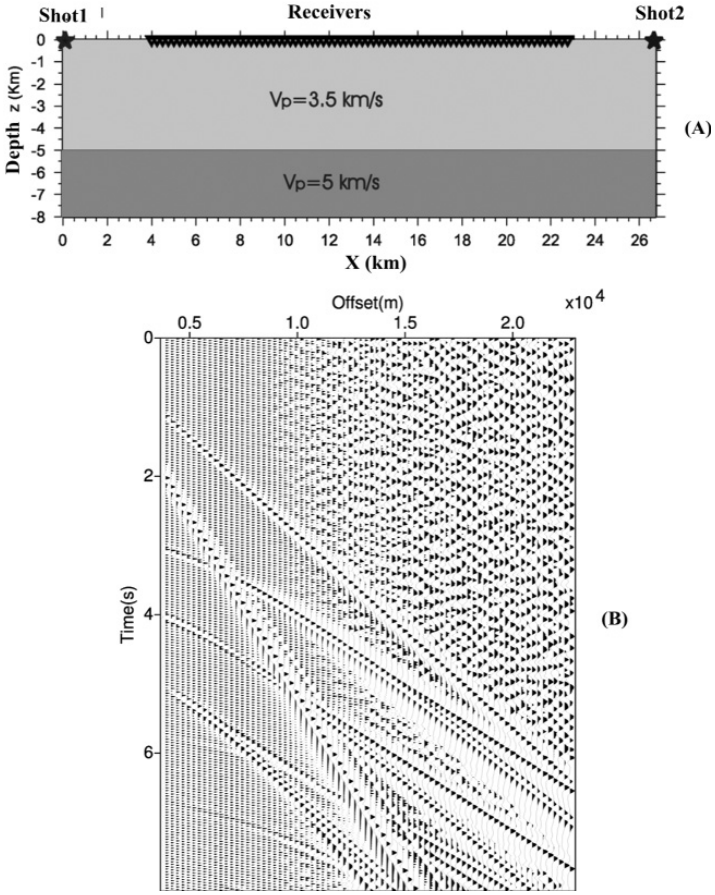

Fig. 7. Adopted model (A) for generation of synthetic seismograms (B). The triangles show the locations of the receivers and the stars show the positions of the sources (A). The synthetic common source gather section (B) shows only the first 10 s of the simulated traces relative to shot 1. The traces are normalized for the maximum trace values and they are filtered with an AGC filter on a window of 0.5 s. No filters were applied to the traces during the inversions.
You can see this figure in color on page 200.

The retrieved interface models are shown in Figure 8. Following the multiscale strategy, the inversion begins with the position search of the model defined from two single nodes, these are searched for in depths ranging from 2 km to 6 km. All of the obtained interfaces are horizontal and are approximately located at 5.1 km in depth. The retrieved depth interface locations are very close to the real depth of the interface (5 km; Figure 8). The possible cause of the discrepancy between these two values could be the Vp value assumed during

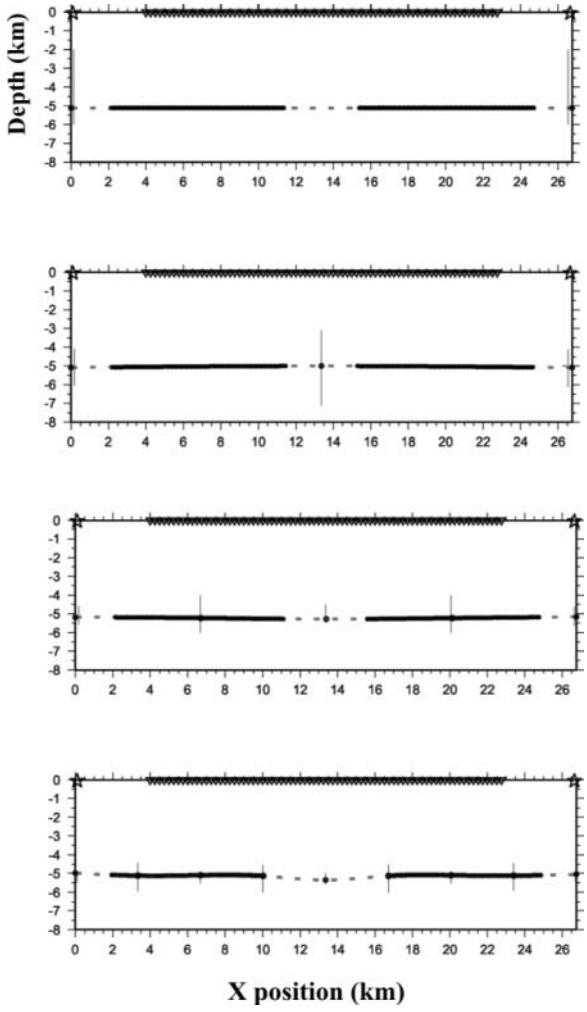

Fig. 8. Interfaces obtained with inversions of synthetic traces. The interface models (dotted line) were obtained performing a succession of four inversion runs with an increasing number of interface nodes (solid circles). The dots on the interface model are the impact points of seismic rays; the vertical bars are the intervals of search of the nodes.

the inversion; this was obtained on the basis of a normal move-out analysis that was performed on the synthetic section and it is greater than 0.1 km/s with respect to the real Vp value. The models obtained in the different singular steps (increasing the number of nodes; Figure 8) are very similar, and they are all in the same position. This is due to the simplicity of the propagation model adopted: only two nodes are enough to represent the complexities of the real interface.

The reliability of the retrieved model can be verified with the construction of the seismic panels obtained by the seismograms that are corrected for the calculated reflection travel times. With no error in the location and shape of the interface, the modelled reflection events should align at 0 s and should show a lateral coherence on the panels. Therefore, the reliability of the determined interface can be verified by measuring the alignment of the reflection events on the panel by the semblance value assumed on the traces corrected for the estimated travel times. Figure 9 shows an example of the time move-out panel that was obtained by correcting the traces for the retrieved nine-node model. The alignment and the wave-form coherence of the reflected phase are excellent in all of the panels. The phase alignment and the coherence are given by the semblance trace, which clearly shows a high peak at 0 s.

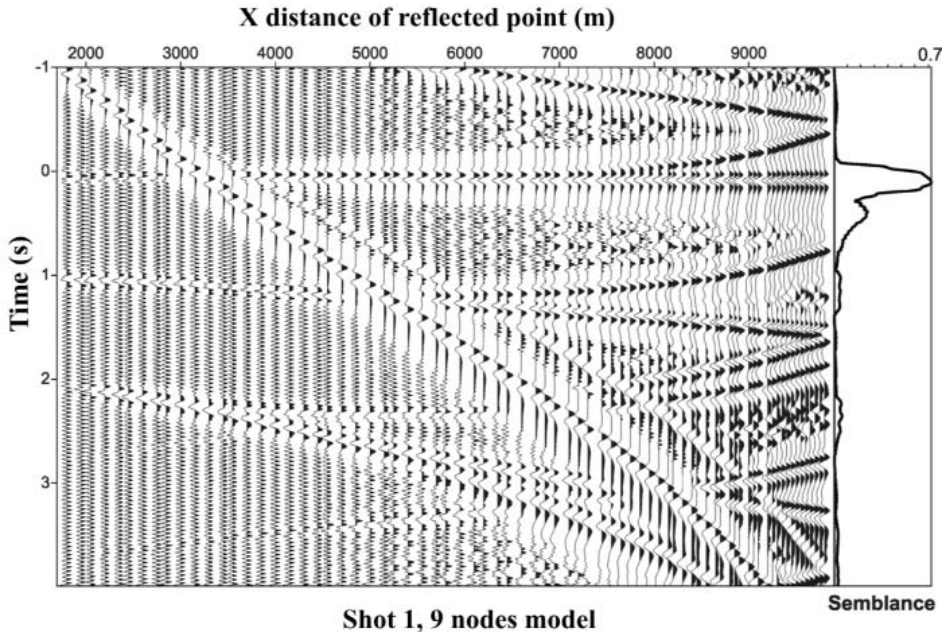

Fig. 9. Time moved-out section. The traces are corrected for the estimated travel times of the modelled reflected phase by the 17-node interface show in Figure 8. The horizontal semblance value of the traces allows the measuring of the alignment and coherence of the modelled phase.

Application to real active seismic data

The 2D non-linear inversion method was applied to a subset of data collected during the active seismic experiments performed in September 2001 in the gulfs of Naples and Pozzuoli in the framework of the SERAPIS project (Judenherc and Zollo, 2004) (Figure 10). The data (475 seismograms) used for the inversions were recorded by ocean-bottom system (OBS) O48 for the shots situated in a band of 250 m centred at the QUR line (Figure 10).

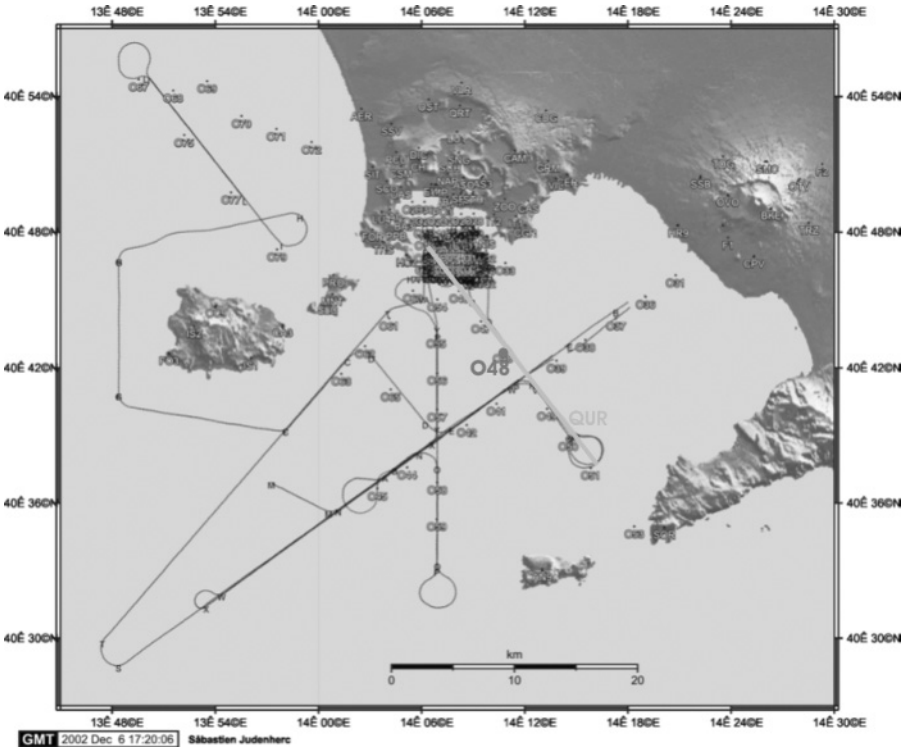

Fig. 10. Station and shot map of the SERAPIS experiment. The lines show the positions of the shots (more than 5,000 air-gun shots at spacings of about 125 m). The dots show the position of the stations (60 on-land stations, and 72 ocean-bottom seismographs).
You can see this figure in color on page 200.

The assumed background velocity model is composed of one layer over the half space. The upper layer extends from 0 to 1.1 km (b.s.l.) with a Vp of 1.9 km/s. The half-space Vp is assumed to be 3.4 km/s. These velocities were assigned following the NMO correction on the CRG section (Figure 11).

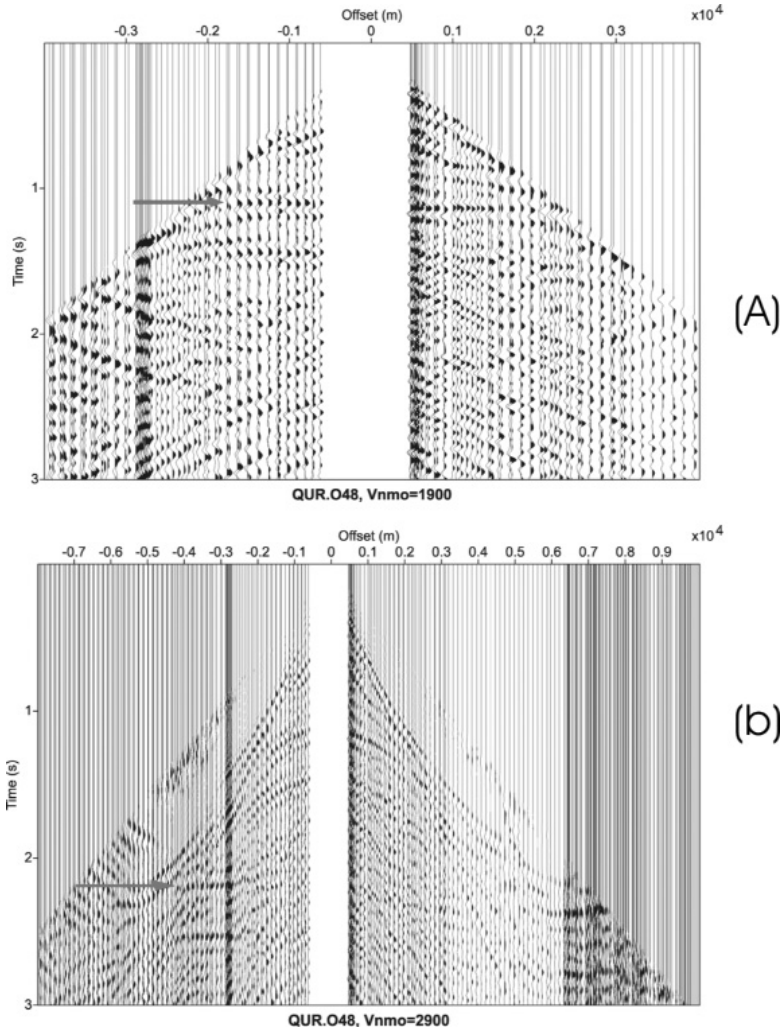

Fig. 11. Normal move-out corrections on traces recorded by OBS 048. The correction shows two clear phases: the first is well corrected by an NMO velocity of 1,900 m/s [indicated with arrows in (a)], and the second is flat for a velocity of 2,900 m/s [arrows in(b)].

A succession of five interface models parametrized by 2, 3, 5, 9 and 17 nodes were progressively inverted (Figure 12). Moving from a small to a larger number of interface position nodes, we always observed an increase in the final value of the semblance function. The semblance plot (Figure 13) shows a CRG section that was corrected for the estimated travel times on the maximum semblance interface with 17 nodes. The phase alignment and coherence are shown by the high horizontal semblance values of the traces, which clearly show a coherent signal at 0 s.

The determined maximum semblance interface (17-node interface model) is interpreted as the top of a carbonatic platform. This result is consistent with the tomographic sections obtained from the tomographic inversion of the first arrivals (Judenherc, 2004).

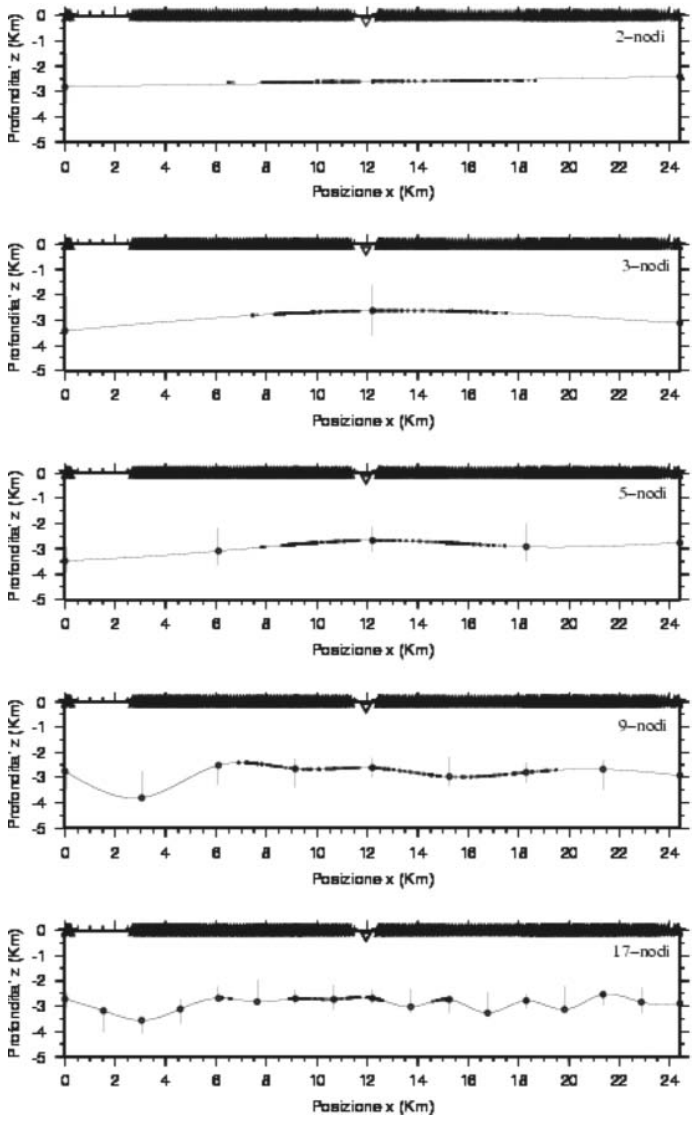

Fig. 12. Maximum semblance interface models obtained by performing a succession of five inversion runs with an increasing number of interface nodes (solid circles). The interface inversion technique is applied to over 475 seismograms recorded by the O48 receiver (triangle) for shots (stars) by QUR profile (Figure 10).

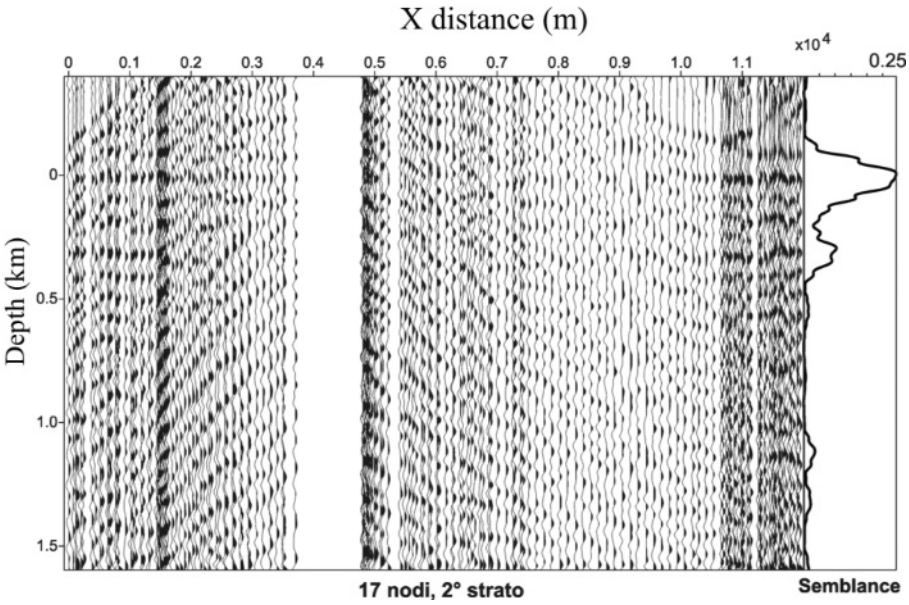

Fig. 13. Time moved-out section. The traces are corrected for the estimated travel times of the modelled reflected phase by the 17-node interface show in Figure 4. The horizontal semblance value of the traces allows the measurement of the alignment and coherence of the modelled phases.

Discussion and conclusions

We have presented two methods to invert the passive (the first method) and active (the second method) seismic reflection data. The described methodologies can be considered as useful tools for the identification and location of the depths of shallow crustal discontinuities when microearthquake records or active seismic data are used. Working with earthquake sources offers the advantage that unlike conventional reflection seismics, the sources are located within the investigated medium and they have larger and more strongly coupled energies than active sources, probing into the deeper crust. Furthermore, earthquakes can provide a much broader frequency bandwidth and represent far more efficient generators of shear waves than controlled sources. The main drawback is that the uncertainties of the estimates of source parameters (origin time, source location, fault mechanism) can influence the quality of the stack, thus affecting the accuracy of the interface depth. There are ways of minimizing these inherent difficulties, by considering some additional corrections and by selecting an appropriate earthquakes data set (James et al., 1987) and using active and passive seismic data at the same time.
Despite the assumed simplicity of the propagation medium, this technique has been proven to be robust and efficient for the search and first-order model-

ling of secondary arrivals on microearthquake records. The shape and width of the semblance function peak is a measure of the uncertainty of the interface depth, since a narrow semblance curve indicates a well-constrained interface depth. It also provides an estimate for the phase-timing error, which is related to unknown path and source effects. We applied this methodology to P-to-P and S-to-P waves observed on local earthquake records acquired by the surveillance seismic network operating on the Mt. Vesuvius volcano. Recent studies using reflected/converted wave fields of crustal discontinuities beneath the Mt. Vesuvius volcano were reported by Auger et al. (2001) using an active seismic data set. Based on the modelling of wave amplitudes as a function of the incidence angle, this study identified a major seismic discontinuity at about 8 km in depth, characterized by a negative velocity contrast (from 6 km/s to less than 4 km/s for P waves, and from 3.5 km/s to less than 1.0 km/s for S waves).

Our analysis of microearthquake records confirms this evidence, although it provides a slightly greater value for the interface depth (9 km) beneath the volcanic complex. This discrepancy can be attributed to the use of a simplified crustal model, whereas in the Auger et al. (2001) study, accurate static corrections were applied to the data to account for the lateral variation of the shallow velocity structure. Based on the measured velocity contrast, Auger et al. (2001) interpreted the reflector as the top of a midcrust, sill-like magmatic reservoir beneath the volcanic complex, with a lateral extent of at least 400 km^2.

This result, and the P and S velocities estimated by Auger et al. (2001), suggest a partially molten body, consistent with highly fractured rock with diffusive melt. Several observations of midcrust discontinuities associated with magmatic reservoirs beneath volcanoes have been made worldwide, based on seismic-data modelling. Beneath the Nikko-Shirane volcano (the Northeast Japanese arc), a midcrust reflector was identified at 8-15 km in depth with a lateral extension of about 15x15 km^2, which is interpreted as the top of a low-velocity thin layer of partially melted material (Matsumoto and Hasegawa, 1996). In the volcanic area of Casa Diablo, Long Valley, California, USA, seismic reflections from a 1.5-2-km^2 curved surface have been interpreted as being produced by the roof of a magma chamber at about 7.8 km in depth (Sanders, 1984). The presence of magmatic sills in the depth range of 8-20 km beneath different volcanoes worldwide is attributed to a neutral condition of the magma buoyancy force with the surrounding crust. The uprising of magma from the mantle in an extensional tectonic regime can give rise to thin and wide sill reservoirs in the upper crust (Ryan, 1994; Iyer et al., 1990). The discovery of a deep, sill-like magmatic reservoir beneath Mt. Vesuvius is relevant for the understanding and modelling of possible future eruptive scenarios.

The method presented using inverted active seismic data is tested on synthetic data and it has been used to image the location of a carbonatic platform

under the gulf of Naples. The method is specifically designed for geophysical investigations in complex geological environments where the presence of complex structures makes the standard velocity analysis difficult and degrades the quality of migrated images. Inversion based on coherence measures (semblance) does not require the picking of reflections, thus improving the time performance of the whole procedure and removing the subjectivity of the human operators in the picking procedure.
Our inversion that is based on the maximization of the semblance or on the minimization of the cost function demonstrates with synthetic data that the method is stable and efficient when it is used coupled to a multistep strategy. The interface model that is obtained by application of this inversion method on the SERAPIS data is interpreted as the top of a carbonatic platform, and this result is consistent with the tomographic studies recently published by Judenherc (2004).

References

Amand P., Virieux J. (1995). Non linear inversion of synthetic seismic reflection data by simulated annealing. *65th Ann. Internat. Mtg: Soc. Expl. Geophy. Expanded Abstracts*, 612-5.

Auger E., Gasparini P., Virieux J., Zollo A. (2001). Imaging of a mid-crust high to low seismic discontinuity beneath Mt. Vesuvius. *Science*, 204, 1510-2.

Al-Yahya K. (1989). Velocity analysis by iterative profile migration. *Geophysics*, 54, 718-29.

Balch R. S., Hartse H. E., Sanford A., Lin K. (1997). A new map of the geographic extent of the Socorro mid-crustal magma body. *Bull. Soc. Seism. Am.*, 87, 174-82.

Bernard M.-L., Zamora M. (2000). Mechanical properties of volcanic rocks and their relations to transport properties. *EOS, Trans. Am. Geophys. U.*, 81, Fall Meet. Suppl., Abstract V71A-33.

Boschetti F., Dentith M. C., List R. D. (1996). Inversion of seismic refraction data using genetic algorithms. *Geophysics*, 61, 1715-27.

Coutant O. (1989). Programme de simulation numerique AXITRA. *Res. Report LGIT*, Grenoble.

Gasparini P., Tomoves Working Group (1998). Looking inside Mount Vesuvius. *EOS, Trans. Am. Geophys. U.*, 79, 229-32.

Goldberg X. (1989). Genetic Algoritm in Search, Optimization and Machine Learning. *Addison-Wesley Pub. Co., pp. 432*.

Improta L., Zollo A., Herrero A., Frattini R., Virieux J., Dell'Aversana P. (2002). Seismic imaging of complex structures by nonlinear traveltime inversion of dense wide-angle data: application to a thrust belt. *Geophys. J. Int.*, 151, 264-8.

Iyer H. M. (1992). Seismological detection and delineation of magma chambers:Present status with emphasis on the Western USA, in *Volcanic Seismology*, edited by P. Gasparini, R. Scarpa, K. Aki, Springer-Verlag, pp. 299-338.

Iyer H. M., Evans J. R., Dawson P. B., Stauber D. A., Achauer U. (1990). Differences in magma storage in different volcanic environments as revealed by seismic tomography: silicic volcanic centers and subduction-related volcanoes, in *Magma transport and storage* edited by M.P. Ryan, Wiley, pp. 293-316.

James D., Clarke T., Meyer R. (1987). A study of seismic reflection imaging using microearthquake sources, *Tectonoph.*, 140, 65-79.

Lomax A., Zollo A., Capuano P., Virieux J. (2001). Precise, absoute earthquake location under Somma-Vesuvius volcano using a new 3D velocity model. *Geophys. J. Int.*, 146, 313-31.

Lomax A., Virieux J., Volantand P., Berge C. (2000). Probabilistic earthquake location in 3D and layered models: Introduction to a Metropolis-Gibbs method and comparison with linear locations, in *Advances in seismic event location*, edited by C.H. Thurber, N. Rabinowitz, Kluwer, Amsterdam, pp. 101-134.

Matsumoto S., Hasegawa A. (1996). Distinct S wave reflector in the midcrust beneath Nikko-Shirane volcano in the northeastern Japan arc. *J. Geoph. Res.*, 101, 3067-83.

Naess O. E., Bruland L. (1985). Stacking methods other than simle summation, in *Developments in Geophysical Methods*, 6, 189-223, edited by A.A. Fitch, Elsevier Applied Science Publishers, London.

Neidell N. S., Taner M. S. (1971). Semblance and other coherency measurements for multichannel data. *Geophysics*, 36, 482-97.

Nisii V., Zollo A., Iannaccone G. (2003). Depth of a mid-crustal discontinuity beneath Mt Vesuvius from the stacking of reflected and converted waves on local earthquake records. *Bull. Soc. Seism. Am.*, 94(5), 1842-9.

Podvin P., Lecomte I. (1991). Finite difference computation of traveltimes in very contrasted velocity models: a massively parallel approach and its associated tools. *Geophys. J. Int.*, 105, 271-84.

Ryan M. P. (1994). Neutral-Buoyancy Controlled Magma Transport and Storage in Mid-ocean Ridge Magma Reservoirs and Their Sheeted-Dike Complex: A Summary of Basic Relationships. in *Magmatic Systems*, vol. 2, edited by M.P. Ryan, Academic Press, London, pp. 97-138.

Rinehart E., Sanford A. R. (1981). Upper crustal structure of the Rio Grande Rift near Socorro, New Mexico, from inversion of microearthquake S-wave reflections. *Bull. Soc. Seism. Am.*, 71, 437-50.

Toldi J. L. (1989). Velocity analysis without picking. *Geophysics*, 34, 191-9.

Sambridge M., Drijkoningen G. (1992). Genetic algorithms in seismic waveform inversion. *Geophys. J. Int.*, 109, 323-42.

Sanders C. O. (1984). Location and configuration of magma bodies beneath Long Valley, California, determined from anomalous earthquake signals. *J. Geophys. Res.*, 89, 8287-302.

Sanford A. R., Alptekinand O., Toppozada T. R. (1973). Use of reflection phases on microearthquake seismograms to map an unusual discontinuity beneath the Rio Grande Rift. *Bull. Seism. Soc. Am.*, 63, 2021-34.

Sheriff R. E., Geldart L. P. (1982). Exploration Seismology. *Cambridge University Press*, New York.

Stroujkova A. F., Malin P. E. (2000). A magma mass beneath Casa Diablo? Further evidence from reflected seismic waves. *Bull. Seism. Soc. Am.*, 90, 500-11.

Yilmaz O. (1987). Seismic Data Processing, in *Investigations in Geophysics*, edited by B. Nictzel, Vol. 2, Society of Exploration Geophysicists, Tulsa, Oklahoma.

Yilmaz O., Chambers R. (1984). Migration velocity analisis by wavefield extrapolation. *Geophys.*, 49, 1664-74.

Zollo A., Gasparini P., Virieux J., Le Meur H., De Natale G., Biella G., Boschi E., Capuano P., de Franco R., Dell'Aversana P., De Matteis R., Guerra I., Iannaccone G., Mirabile L., Vilardo G. (1996). Seismic evidence for a low-velocity zone in the upper crust beneath Mount Vesuvius. *Science*, 274, 592-4.

Zollo A., D'Auria L., De Matteis R., Herrero A., Virieux J., Gasparini P. (2002). Bayesian estimation of 2D P-velocity models from active seismic arrival time data: Imaging of the shallow structure of Mt. Vesuvius (Southern Italy). *Geophys. J. Int.*, 151, 556-82.

Zollo A., Marzocchi W., Capuano P., Lomax A., Iannaccone G. (2002). Space and time behaviour of seismic activity al Mt. Vesuvius volcano, Southern Italy. *Bull. Seism. Soc. Am.*, 92(2), 625-40, doi: 10.1785/0120000287.